

**Zeitschrift:** Eclogae Geologicae Helvetiae  
**Herausgeber:** Schweizerische Geologische Gesellschaft  
**Band:** 96 (2003)  
**Heft:** 2

**Artikel:** A new interpretation of the Chasseral magnetic anomaly (Swiss Jura)  
**Autor:** Klingelé, Emile E. / Verdun, Jérôme  
**DOI:** <https://doi.org/10.5169/seals-169019>

### **Nutzungsbedingungen**

Die ETH-Bibliothek ist die Anbieterin der digitalisierten Zeitschriften. Sie besitzt keine Urheberrechte an den Zeitschriften und ist nicht verantwortlich für deren Inhalte. Die Rechte liegen in der Regel bei den Herausgebern beziehungsweise den externen Rechteinhabern. [Siehe Rechtliche Hinweise.](#)

### **Conditions d'utilisation**

L'ETH Library est le fournisseur des revues numérisées. Elle ne détient aucun droit d'auteur sur les revues et n'est pas responsable de leur contenu. En règle générale, les droits sont détenus par les éditeurs ou les détenteurs de droits externes. [Voir Informations légales.](#)

### **Terms of use**

The ETH Library is the provider of the digitised journals. It does not own any copyrights to the journals and is not responsible for their content. The rights usually lie with the publishers or the external rights holders. [See Legal notice.](#)

**Download PDF:** 29.03.2025

**ETH-Bibliothek Zürich, E-Periodica, <https://www.e-periodica.ch>**

# A new interpretation of the Chasseral magnetic anomaly (Swiss Jura)

EMILE E. KLINGELÉ<sup>1</sup> & JERÔME VERDUN

*Key words:* Swiss Jura, Chasseral, airborne and ground magnetic interpretation

## ABSTRACT

The magnetic total field anomaly of Chasseral (Swiss Jura Mountains) has been re-interpreted by means of Euler's deconvolution, reduction to the pole and two and three-dimensional modelling. This interpretation suggests that the anomaly is produced by a body of pear's shape of around 50 km length and 30 km maximal width, oriented roughly WNW-ESE, the thicker part lying between the Doubs river, the Chasseral culmination and the city of La Chaux-de-Fonds. The model of the disturbing body is formed of compartments vertically delimited extending from 6 km to 2 km below sea level.

A structure of blocks of the disturbing body is strongly supported by the results of the Euler's deconvolution. The susceptibilities of these blocks range from 0.010 to 0.025 SI, the value of 0.015 SI being the most common. The comparison between the proposed model and the depth to the magnetic basement of this region suggests that the disturbing body lies inside the crystalline basement. Another hypothesis could be that the body represents the bottom of an old trough.

## RESUME

L'anomalie magnétique du Chasseral (Jura Suisse) a été réinterprétée en utilisant la déconvolution d'Euler, la réduction au pôle et des modélisations en deux et trois dimensions. Cette interprétation suggère que l'anomalie est produite par un corps ayant une forme de poire, d'une longueur d'environ 50 km pour une largeur maximum de 30 km, orientée WNW-ESE et ayant sa partie la plus large centrée dans un triangle formé par le Doubs, le Chasseral et la ville de La Chaux-de-Fonds. Le modèle proposé est formé de compartiments verticaux dont les profondeurs varient de 6.0 km à 2.5 km sous le niveau de la mer. Les résultats de la déconvolution d'Euler attestent de façon concluante, de la structure en blocs du corps. Les susceptibilités de ces blocs se situent entre 0.010 SI et 0.025 SI, la valeur de 0.015 étant la plus commune. Une comparaison entre les profondeurs du soubassement magnétique de la région et du modèle obtenu suggère que le corps est situé à l'intérieur du soubassement cristallin. Une autre hypothèse serait que ce corps soit le fond d'un ancien fossé.

## Introduction

In the year 1980 the Swiss Geophysical Commission published its first three geophysical maps of Switzerland at the scale of 1:500'000. Two of these geomagnetic maps produced by G. Fischer and P.-A. Schnegg of the Cantonal Observatory of Neuchâtel (Fischer & Schnegg 1979) show an anomaly of around 100 nT located on the Chasseral culmination of the Swiss Jura Mountains. On these maps this anomaly has an extension of around 30 km in the W-E direction and 10 km in the N-S direction. The anomaly of the declination is around 5' and is almost not visible on the inclination map.

The same anomaly appeared much stronger and with more details after the airborne survey at low altitude over the Swiss Molasse Basin and the Jura Mountains carried out by the Swiss Geophysical Commission between 1978 and 1980. The aim of the present paper is to propose a structural interpretation of this anomaly based on a combination of airborne and ground

magnetic data. The area studied extends between the coordinates 548'000 and 611'000 in the West-East direction and between 188'000 and 250'000 in the South-North direction (Fig. 1).

## Geological setting

The Jura Mountains are formed of a sedimentary series lying over a basement of pre-Triassic age. The formation of the Jura Mountains can be linked to the alpine orogenesis and can be interpreted as the result of a north-westward stamping effect transmitted by the Molasse basin under the pressure of the Alps. (Laubscher 1972)

The sedimentary Mesozoic series were folded after their detachment from the basement due to the Triassic evaporitic formations. Important networks of faults, which can be classified in three families, cross these Mesozoic sedimentary series:

GGL, Institute of Geodesy and Photogrammetry, ETH Zurich  
ETH- Hönggerberg, CH-8093 Zurich, Switzerland. E-mail: klingele@geod.baug.ethz.ch

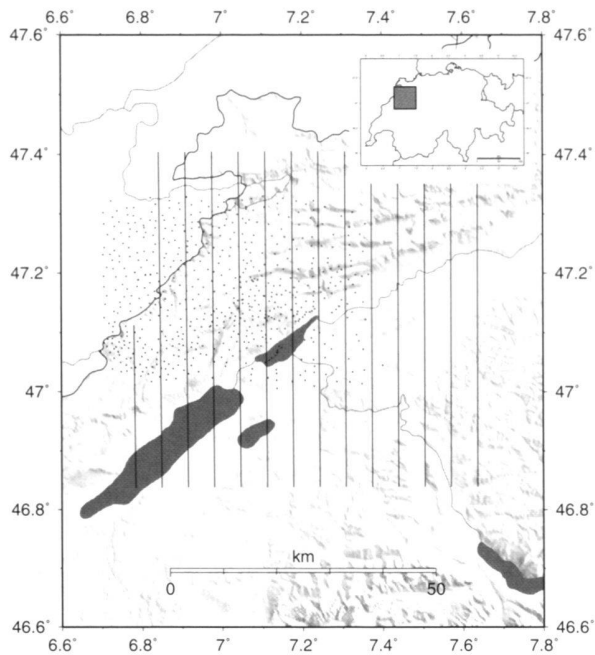


Fig. 1. Map showing the location of the studied area, the locations of the flight lines and the locations of the ground measurement stations.

1. The SW-NE faults called "varisques", probably caused by the re-activation of Variscan-Hercynian structures.
2. The sub-meridian faults, which are part of the large dislocation system which gave rise to the Rhine-Graben.
3. The radial faults, most of them sinistral thrust faults, crossing the folded Jura Mountains, some of them having a prolongation inside the external part of the Jura Mountain like the Pontarlier and Morez faults. They are genetically linked to the folding mechanism, which could have been different from one side to another side of the faults.

The crystalline basement of the Jura Mountains is formed of Paleozoic rocks having experienced the Variscan-Hercynian orogeny of which the structural direction is SW-NE. Its depth increases from the NW to the SE. The information about this basement is scarce. Data come from deep soundings and a few observations made on some outcrops located along the external border of the chain like Vosges Mountains, Serre massif and the Crémieu Island.

The rocks are mostly gneiss, micaschists and granites. A synthesis of the data coming from deep soundings and geophysics (magnetic, gravity, and reflection seismic) resulted in a structural map of the top of the pre-Triassic basement of a part of south-east of France (Debeglia & Gable 1984). This map does not give many details but allows at least to differentiate the categories of geological formations that are present in the upper part of the basement as a function of their magnetic and gravity properties. The seismic data give, in the best case, some

information about the depth of the top of the basement. This map reveals in the region of the external Jura Mountains a granitic basement showing a low magnetic susceptibility and also a low to medium density. This basement is crossed by a series of volcano-sedimentary rocks of Devonian age and by crystalline shales of higher magnetic susceptibility. Structures oriented SW-NE and formed of basic and magmatic rocks with high susceptibility are also present. The zone studied in the present publication is located in the domain of the high chain of the Swiss Jura Mountains. It is mostly formed of limestone of Jurassic to Cretaceous age sometimes covered by Tertiary molasse. This zone extends as far as the region of Franche-Comté in France. The principal summit of this region is the Chasseral which culminates at 1607 m above sea level and which has given its name to the anomaly studied here.

### The airborne data

Between 1978 and 1981 the Swiss Geophysical Commission carried out two airborne magnetic surveys over the Swiss territory (Klingelé 1983, 1986). The measurements were performed along straight lines oriented North-South, with a line spacing of 5000 m and flown at respectively 5000 m a.s.l. over the whole territory and 6000 feet a.s.l. for the part covering the Molasse basin and the Jura Mountains. Control lines (cross lines) were also flown but in West-East direction and with a line spacing of 20'000 m. For this survey a Twin-Otter DeHavilland aircraft belonging to the Swiss Federal Office of Topography was used. The aircraft was equipped with a precession magnetometer GeoMetrics G803 measuring the total magnetic field at 1 second sampling rate with a resolution of 0.25 nT. The sensor of the instrument was towed in a bird 30 m behind the aircraft.

During the measurement campaigns a base station was installed near Zurich. This station recorded the total magnetic field at the same sampling rate as the airborne instrument. The data collected by this station as well as those provided by the magnetic observatory of Neuchâtel (AMOS station) were used for correcting the measurements for the secular and diurnal variations of the magnetic field and also for reducing the data to the same reference time (1980.5). A regional field has been subtracted from the data in order to identify anomalies suitable for the interpretation. This regional field was calculated by using the International Geomagnetic Reference Field for the year 1980.5. Finally the data were gridded with a mesh size of 1 km and the part of interest for the present work was extracted from the global grid. A map of the anomaly field for the low altitude survey is presented in figure 2a.

### The ground data

The ground magnetic data were acquired during four summer campaigns between 1986 and 1990 by the Laboratory of Petrophysics of the University of Geneva in collaboration with the Institute of Geophysics of the University of Lausanne (Risnes

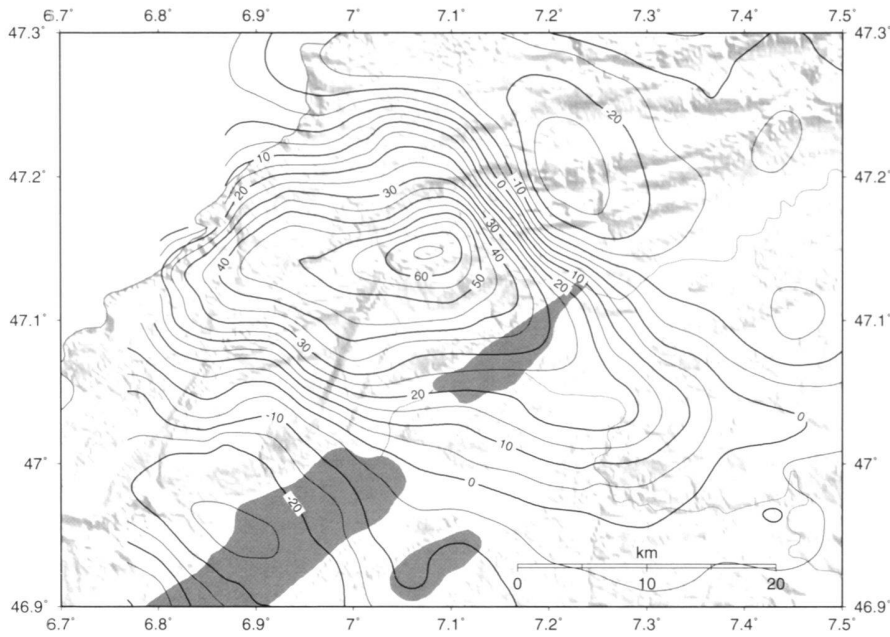


Fig. 2a. Map of the total field residual anomalies obtained from the airborne magnetic data. The units are [nT]

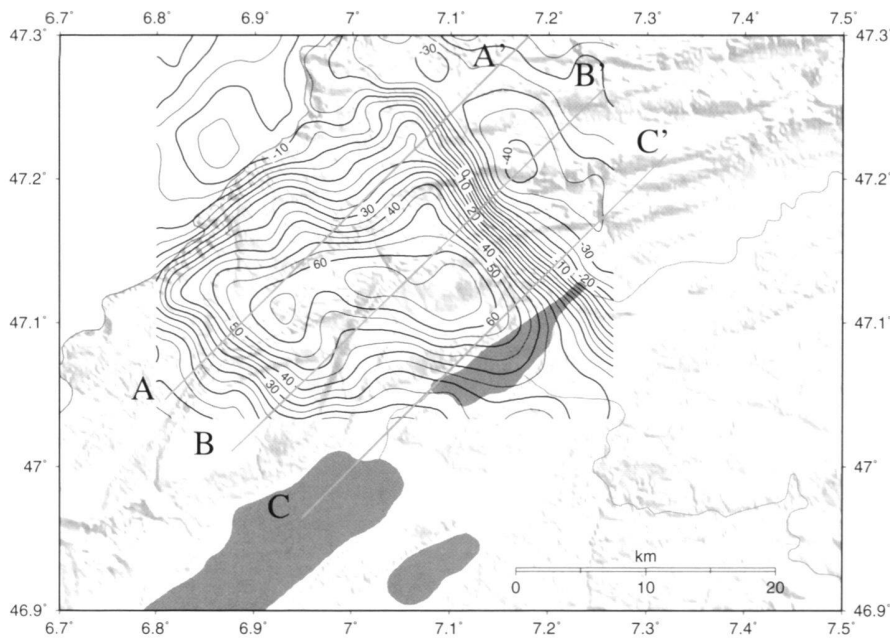


Fig. 2b. Map of the total field residual anomalies obtained from the ground magnetic data. The lines marked AA', BB' and CC' correspond to the profiles interpreted in two dimensions in figures 6a, 6b and 6c. The units are [nT]

et al. 1993). Six hundred and twenty seven points were measured with a precession magnetometer Geometrics G-856 having a resolution of 0.1 nT. Throughout the survey a second magnetometer was installed in the middle of the area, measuring the magnetic field constantly for removing the effects of the diurnal variations. After the end of the measuring campaigns the data were reduced to the 1st of September 1986 cor-

responding to the beginning of the measurements. In order to get a real magnetic anomaly a reference field has been subtracted from the reduced data. The reference field was the IGRF 1985 computed for the mean altitude of the survey, which is 1000 m a.s.l. and for the co-ordinates corresponding to each measurement point. This field is represented by a linear function having a horizontal North-South gradient of 2.7

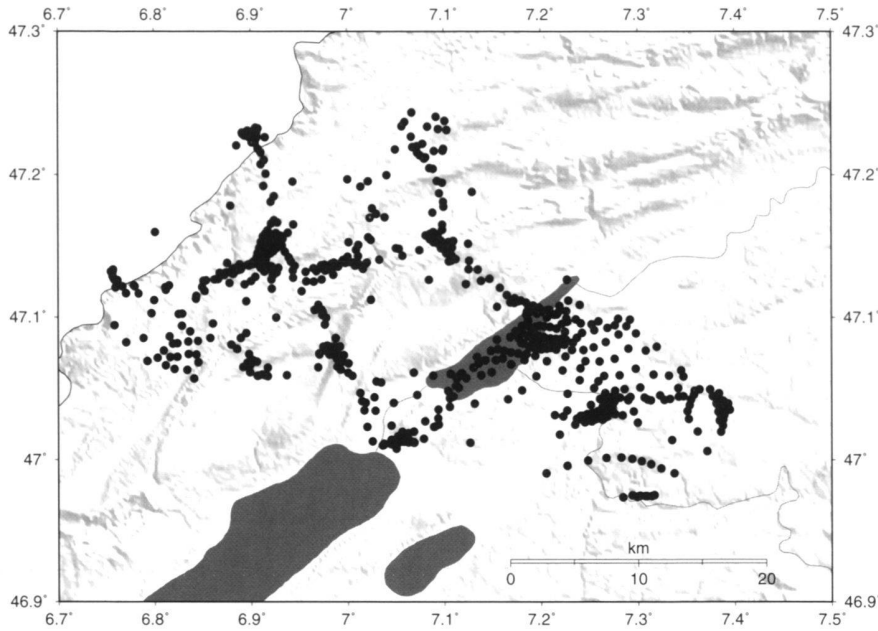


Fig. 3. Map showing the locations of the susceptibility discontinuities obtained by the 3D EULDPH deconvolution.

nT/km and a horizontal gradient East-West of 0.6 nT/km. For the present study the data of the residual field were re-interpolated for producing a map covering more or less the same area as the airborne survey and centred on the anomaly. This map is limited by the co-ordinates 552000 and 589800 in the W-E direction and by the co-ordinates 206400 and 244200 in the S-N direction. These limits were set in order to obtain a matrix of 64 by 64 required for a processing using the Fast Fourier Transform.

The map of the residual field (Fig. 2b) shows a well-defined anomaly having a positive part of 65 nT and a negative part of -40 nT, giving a total amplitude on the order of 100 nT. The locations of the measurement points are shown on figure 1 together with the flight lines of the airborne survey.

### Theory

An earlier interpretation of the airborne data produced a map of the depth to magnetic basement under the Molasse basin and the Jura Mountains (Klingelé & Mueller, 1987). This map results on the one hand from the interpretation of the depths obtained by the method of Treitel et al. (1971) applied to the data of the flight lines and on the other hand from the available data from wells. This paper presents a new interpretation based on the combination of results obtained by means of an integrated application of the analytic signal method (Nabighian 1972,1974; Green & Stanley 1975) and the Euler homogeneity equation method in three dimensions (Thompson 1982; Reid et al. 1990) as well as with a part of the earlier results.

The amplitude of the analytic signal is defined as the

square root of the sum of the square of the first horizontal derivatives and the square of the first vertical derivative of the field, the second being multiplied by the imaginary value  $j$ .

$$|A(x,y)| = \left[ \left( \frac{\delta F}{\delta x} \right)^2 + \left( \frac{\delta F}{\delta y} \right)^2 + \left( j \frac{\delta F}{\delta z} \right)^2 \right]^{\frac{1}{2}}$$

The amplitude of the analytic signal has the property to show maxima at the vertical of the corners of a disturbing body of polygonal cross section. From two or more points of the curve it is also possible to solve for the depth and the slope of a contact. However the method is effective in cases of structures that have two-dimensional characters.

The EULER deconvolution technique also known as EULDPH (Thompson 1982) is based on the property of homogenous functions such as gravity and magnetic fields (a function is called homogenous if the following relationship holds  $f(tx, ty, tz) = t^n f(x, y, z)$ ). Considering a point source located at the point  $x_0, y_0, z_0$  relative to the surface of measurement the magnetic intensity of this source can be expressed by:

$$\Delta F(x, y, z) = f[(x - x_0), (y - y_0), z]$$

The Euler's equation of the above equation can be written as:

$$(x - x_0) \frac{\delta \Delta F}{\delta x} + (y - y_0) \frac{\delta \Delta F}{\delta y} - z_0 \frac{\delta \Delta F}{\delta z} = -N \Delta F$$

The value of  $N$ , called the structural index, depends on the kind of structure producing the anomaly and it is obtained empirically by trial and error. The most used indexes are: 1.0 for a

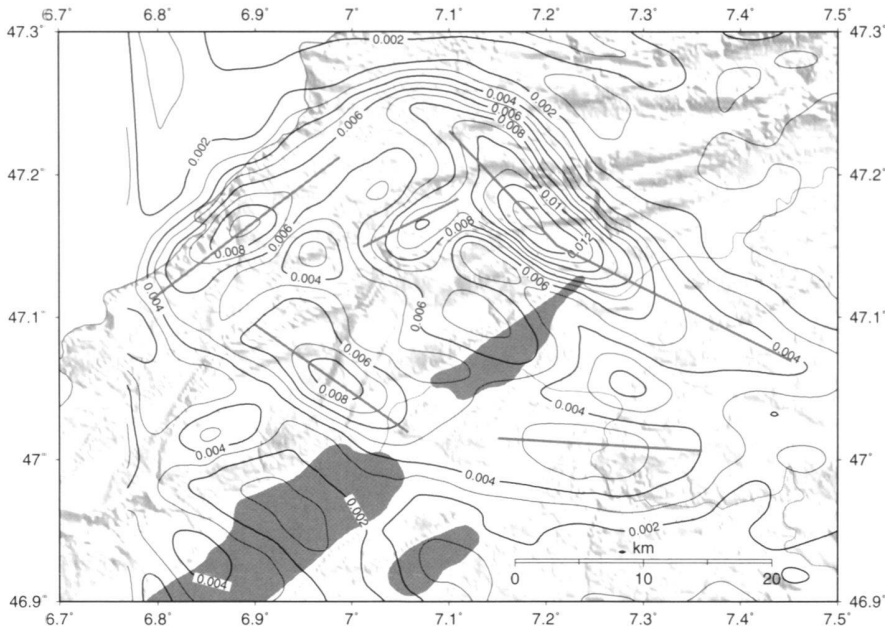


Fig. 4. Map showing the locations of the maximum of the radial horizontal derivative of the residual field anomaly after the reduction to the pole. The units are [nT/m]

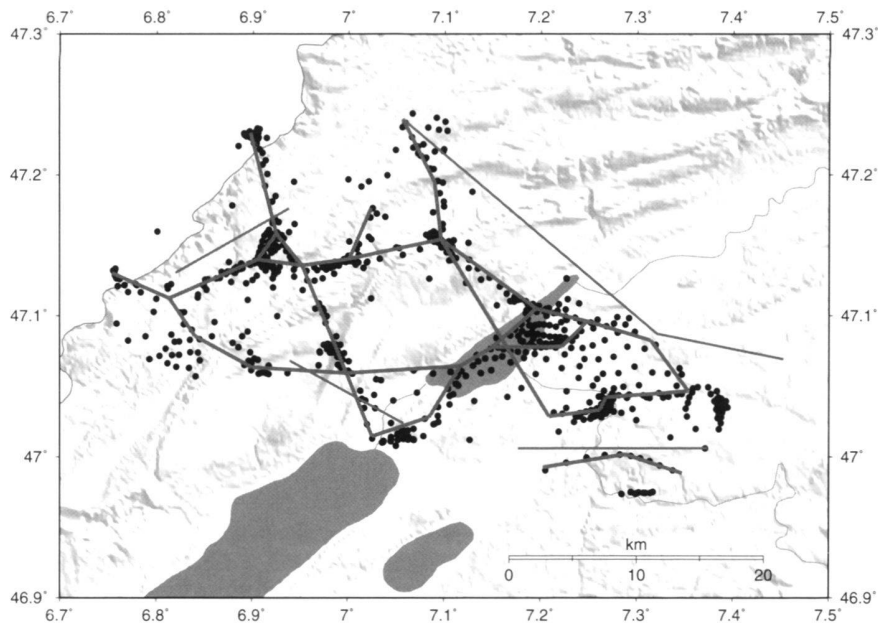


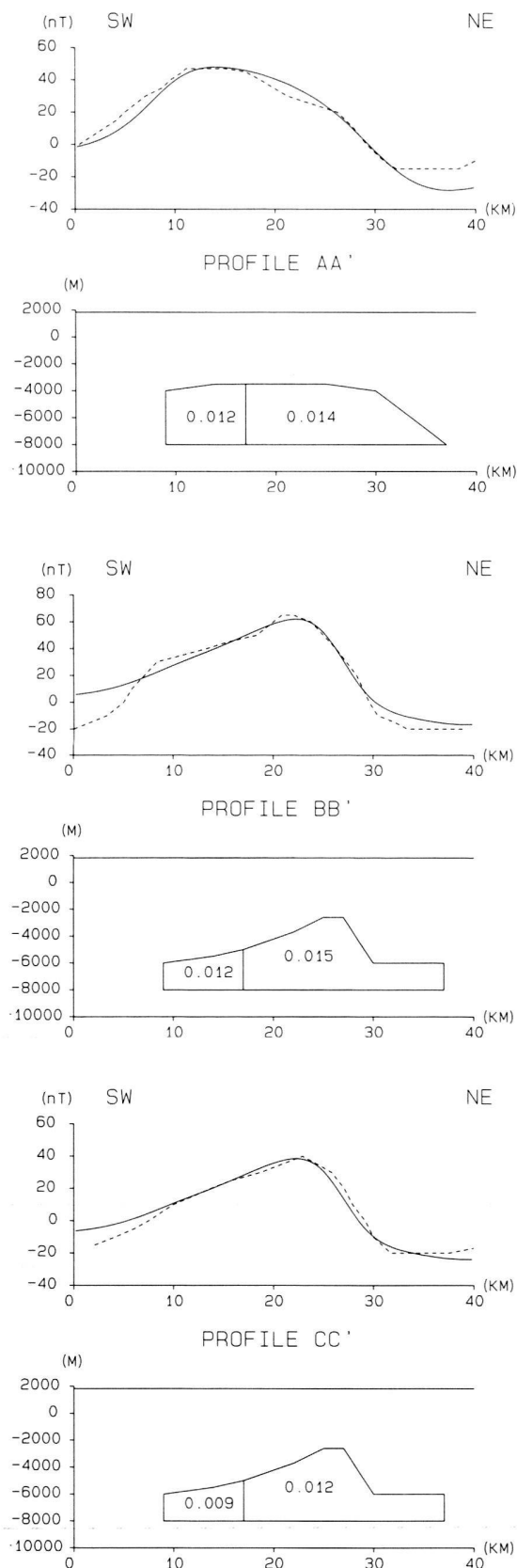
Fig. 5. Map showing the combined interpretation of the horizontal discontinuities obtained by EULDPH deconvolution and obtained from the maximum of the radial horizontal derivative.

line of poles, 2.0 for a point pole or a line of dipoles, and 3.0 for a point dipole.

Because the gradient of the residual field can be easily computed by means of a Fourier Transform the three co-ordinates  $x_0, y_0, z_0$  can be obtained by solving a linear system of three equations involving three measured points. In practice the technique is applied systematically to each point of a grid-

ded map keeping the structural index constant. The procedure is done for different values of the structural index  $N$ . From the cluster of solutions only the values that fulfill a statistical criterion, for example the deviation of a given  $\epsilon$  value around the mean value, are kept and used.

Both the analytic signal and the Euler's deconvolution methods have the common advantage of not requiring any



knowledge of the value of the susceptibilities themselves. Often the analytic signal curve is not perfectly symmetrical, indicating the presence of nearby anomalies, in which case it can only be used to indicate the position of the magnetic discontinuities. Since numerous small interfering anomalies can be often recognized in the interpreted maps, the analytic signal method is preferentially used to find the horizontal location of magnetic discontinuities and/or to better define the operators used in the Euler deconvolution.

### The interpretation of the airborne and ground magnetic data

In both interpretative methods the data require to be on a horizontal plane, thus the interpretation itself was done with the airborne data and the results checked with the ground data. First, the analytic signal technique was applied in order to delineate the most important contacts. Then the EULDPH technique was applied with different deconvolution windows and different structural indexes. Finally the solutions obtained with a structural index of 1 and a window of 7 points were kept and mapped. The solutions on the x,y plane (Fig. 3) show some very interesting features that can be interpreted as limits between different blocks of different depth or/and different susceptibilities. Some solutions are clearly aligned along straight lines while others are more difficult to rely to lines of any shape. Our interpretation in terms of limits between magnetic blocks is presented in figure 5. Unfortunately the EULDPH method is not able to find contacts which are very deep or are masked by stronger susceptibility or depth discontinuities. Therefore, it is possible that the map of the solutions does not show all the contacts forming the disturbing body.

In order to ensure that the three dimensional modelling can be performed with as much contacts as possible we computed the radial horizontal derivative

$$\frac{\delta F}{\delta R} = \left[ \left( \frac{\delta F}{\delta x} \right)^2 + \left( \frac{\delta F}{\delta y} \right)^2 \right]^{0.5}$$

of the anomaly field reduced to the pole. The maxima of this field generally show contacts that cannot be detected by the Euler deconvolution. This appears clearly on figure 4 on which some supposed (and proved later) contacts are visible outside the cluster of the solutions of the Euler deconvolution. Figure 5 shows the combined interpretation of the EULDPH and of the maximum of  $\delta F/\delta H$  in terms of horizontal susceptibility discontinuities.

Our final goal being to present a three-dimensional model of the body some knowledge about depths, susceptibilities and the approximate shape of the disturbing body are needed to begin the modelling. In order to get this information a two-di-

Fig. 6. Results of the two-dimensional modelling along the profiles AA', BB' and CC' of figure 2b and having used as start model for the three dimensional modelling.

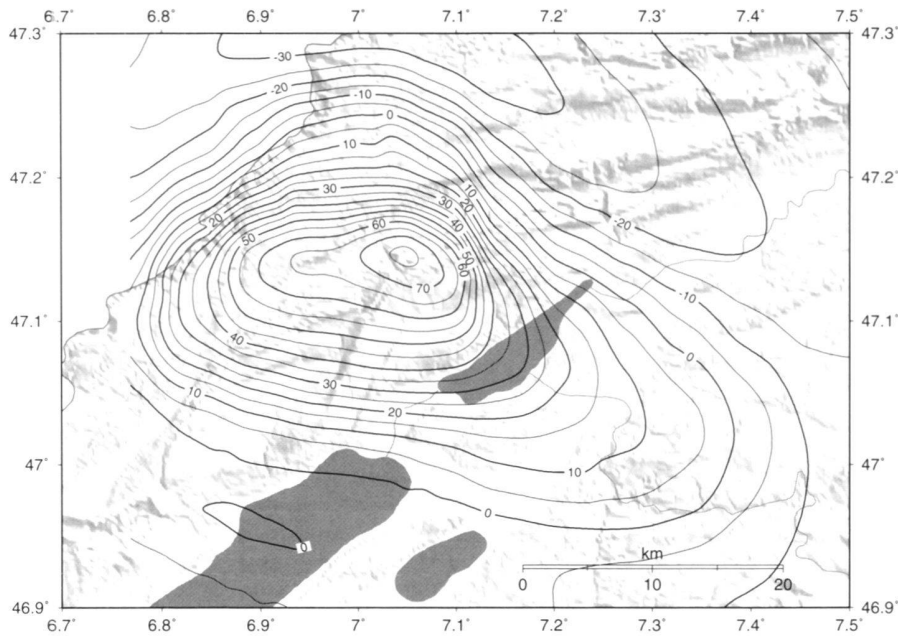


Fig. 7a. Effects of the final solution of the trial and error 3D modelling computed at flight altitude. The units are [nT]

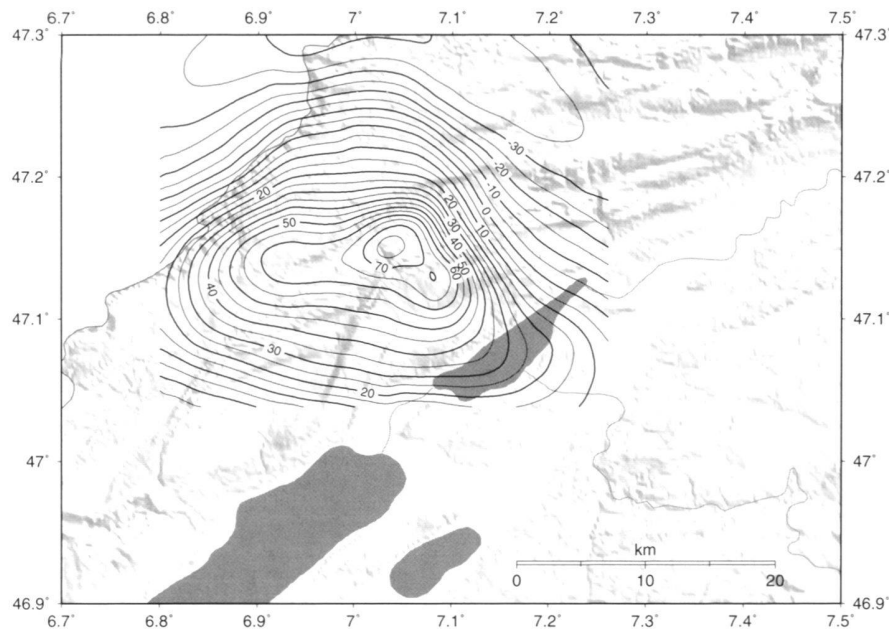


Fig. 7b. Effects of the final solution of the trial and error 3D modelling computed at the locations of the ground stations. The units are [nT] The map has been drawn from a grid obtained by means of a minimal curvature interpolation.

mensional modelling was performed along three profiles (fig 2b) crossing the structure perpendicularly and using as initial values some points of the interpretation given by Risnes et al. (1992). The final two-dimensional models were created by trial and error based on the algorithm of Talwani (1964). The result of this modelling is shown in figure 6. The mean depths obtained from this modelling were given to the corresponding blocks defined by our interpretation of the Euler's deconvolu-

tion results. It should be noted that these depths were good enough for an initial model but much too inaccurate for deriving a final model due to the strong three-dimensional character of the anomaly.

Finally the three-dimensional modelling was performed by trial and error by gently modifying the locations of the corners, by slightly changing the susceptibility of each block and mostly by changing their depth. For the computation the en-

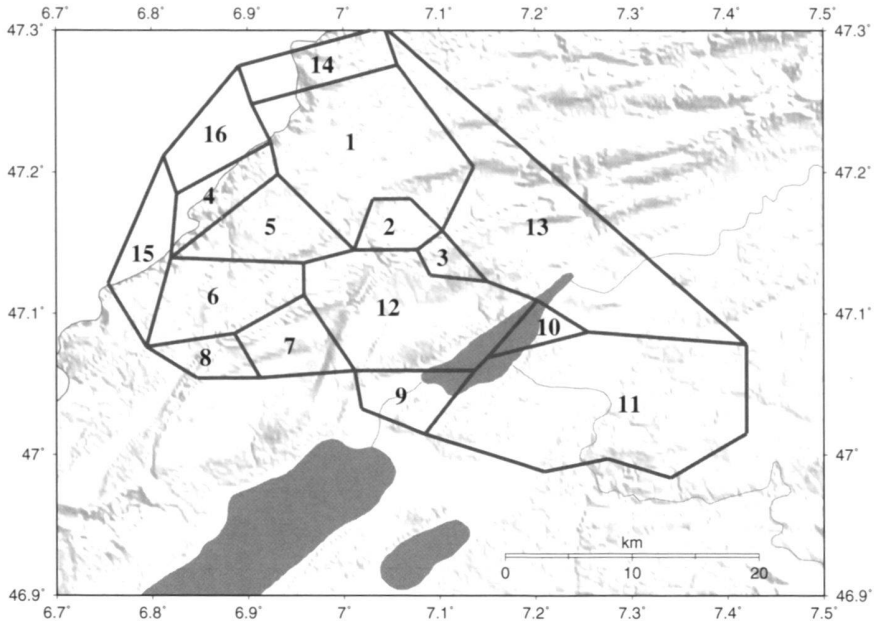


Fig. 8a. Map showing the locations of the blocs forming the disturbing body producing the anomaly of Chasseral. The numbers correspond to those of table 1.

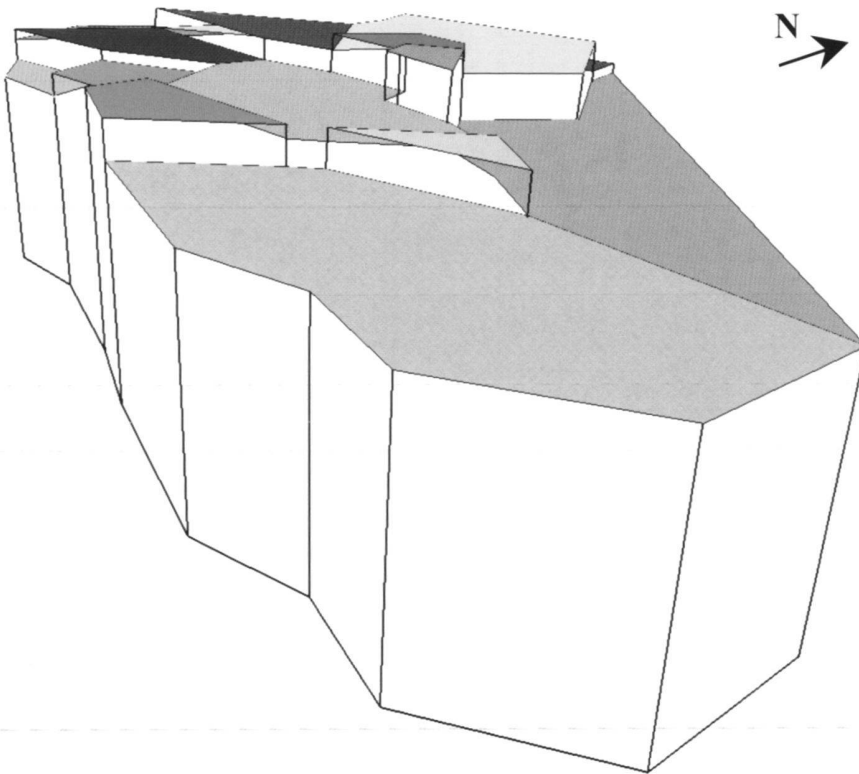


Fig. 8b. Three dimensional view of the disturbing body obtained by a combined interpretation of the airborne and ground residual anomalies. The colours are of arbitrary choice and serve only to facilitate the understanding the three dimensional character of the body.

Tab. 1. Results of the three-dimensional modeling. The block's numbering corresponds to the one of figure 8a.

| Blocks | Depths of the top [m] | Susceptibilities [SI units] |
|--------|-----------------------|-----------------------------|
| 1      | -3500.                | 0.015                       |
| 2      | -2800.                | 0.020                       |
| 3      | -2500.                | 0.025                       |
| 4      | -4500.                | 0.015                       |
| 5      | -3500.                | 0.025                       |
| 6      | -4500.                | 0.015                       |
| 7      | -5000.                | 0.015                       |
| 8      | -6000.                | 0.000                       |
| 9      | -6000.                | 0.015                       |
| 10     | -4000.                | 0.015                       |
| 11     | -5500.                | 0.010                       |
| 12     | -4500.                | 0.015                       |
| 13     | -5500.                | 0.015                       |
| 14     | -5000.                | 0.015                       |
| 15     | -5000.                | 0.015                       |
| 16     | -5000.                | 0.015                       |

tire area was decomposed in vertical prisms of square section and of infinite depth extent and having their top at the depth attributed to the corresponding block. The effect of the inductive field (the Earth's magnetic field) with its intensity, declination and inclination at the time of measurements (Fischer & Schnegg 1979) was computed for each prism and summed at each node of the grid for the airborne data and at the location of each measurement point for the ground data. Then the results were compared with the experimental values and modified if they were not judged good enough. In order to find a satisfactory fit between the experimental anomaly and the computed one some blocks had to be added to the first model. It should be noted that the remanent magnetisation was not taken into account in this procedure. These computations were carried out for the airborne data and for the ground data.

The results of these computations are shown in figures 7a and 7b and the final model with the limits of the different blocks with their depths and their susceptibilities is shown in figure 8a. In order to have an understanding of the three-dimensional character of the disturbing body, a perspective view of the model is presented in figure 8b. One can see that the measured and the computed anomalies match quite well: their maximums are located at the same place and the locations of the zero-lines differ only a few nT. The small horizontal fluctuations of the measured field cannot be modelled with a disturbing body lying at some kilometres depth.

A summary of the mean depths and the susceptibilities is given in table 1.

## Conclusions

The total field magnetic anomaly of Chasseral (Swiss Jura Mountains) is probably produced by a body of pear-shaped outline of around 50 km length and 30 km maximal width, oriented roughly WNW-ESE, the thicker part lying between the Doubs river, the Chasseral culmination and the city of La-Chaux-de-Fonds. The disturbing body is formed of vertically delimited compartments, extending from 6 km to 2 km below sea level. The susceptibilities of these compartments range from 0.010 to 0.025 SI, the value of 0.015 SI being the most common. The block structure of the disturbing body is strongly supported by the results of the Euler deconvolution therefore it has been adopted. The results of the modelling (Table 1 and figures 9a and 9b) compared with the results of the Euler's deconvolution show some small discrepancies or features that cannot be readily explained. For example the solutions in the south-eastern part of the body (block 11) cannot be taken into account in the modelling. The limits between blocks 4 and 5, 4 and 16, 4 and 15 as well as 15 and 16 do not appear in the Euler's solutions. On the contrary the easterly limit of block 12, which does not appear in the solutions of the Euler's deconvolution is clearly marked by the horizontal derivative of the field reduced to the pole. Therefore the inclusion of this block in three-dimensional modelling, despite its "ad posteriori" justification, was a right choice. The small differences appearing in the locations of the limits between some blocks could be explained by the fact that in the modelling the limits are taken as vertical while in reality they could be slightly inclined. Other facts that play an important role are the uncertainties about the inclination, the declination and the intensity of the inducing field at the time of measurement. These uncertainties not only influence the results of the modelling, but also the determination of the regional field on which the location and the shape of the residual anomaly depends. But in spite of these minor discrepancies a satisfactory coherence is achieved between the results obtained by different techniques of interpretation and the experimental data.

Comparing the depths of the blocks forming the disturbing body with the depth of the magnetic basement given by Klingele and Mueller (1987) one can conclude that the body producing the magnetic anomaly of Chasseral lies inside the crystalline basement. Contrary to the finding of Risnes et al. (1993) who have seen in this body a Variscan structure, we do not so, particularly due to its orientation. All the orientations of these structures in the map of Debeglia and Gable (1984) are oriented ENE-WSW, which differs by almost 90 degrees from the orientation of the Chasseral body. If we consider that the magnetically blind zone described by Klingelé & Mueller (1987) is due to a very deep trough, then the Chasseral body could be considered as the bottom of the end of this depression. This last idea has to be considered as a pure hypothesis because no other data support it, but it forms a basis for further research.

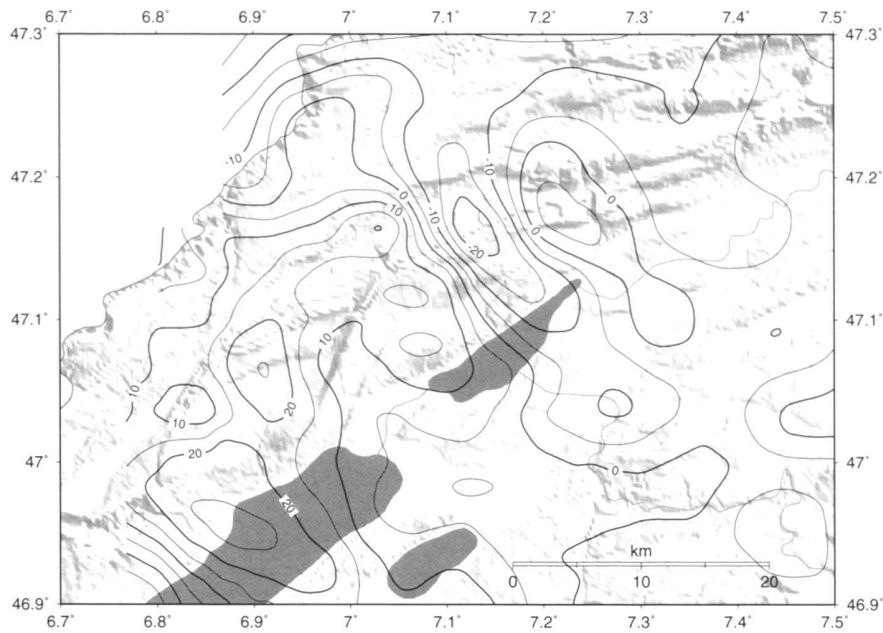


Fig. 9a. Map of the misfit between the experimental airborne data and the effect of the model of figure 8 computed at the flight altitude. The units are [nT]

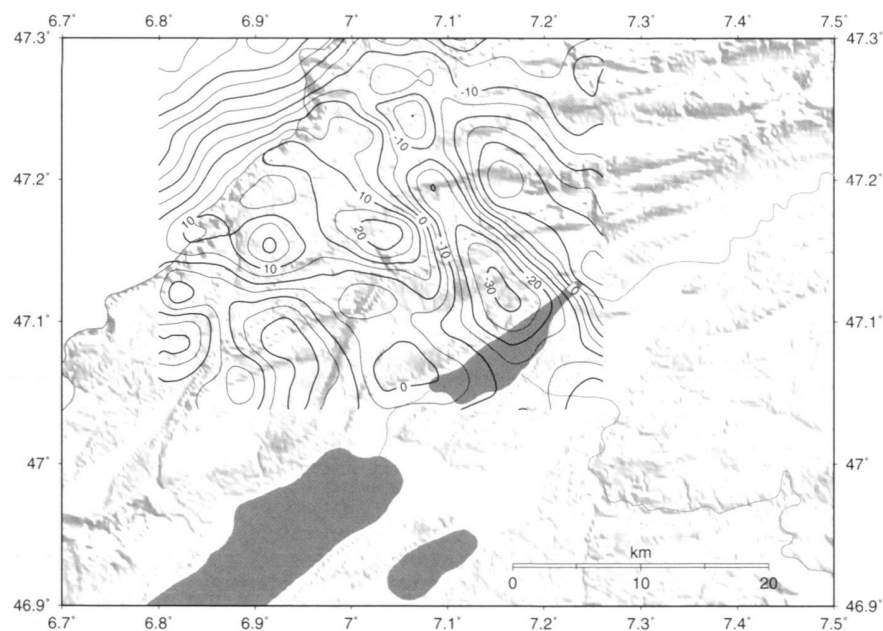


Fig. 9b. Map of the misfit between the experimental ground data and the effect of the model of figure 8 computed at the stations locations. The units are [nT] The map has been drawn from a grid obtained by means of a minimal curvature interpolation.

## REFERENCES

- DEBEGLIA, N. & GABLE R., 1984: Socle Ecorché anté-triasique (planche G3). In: DEBRAND-PASSARD, S. (Ed): Synthèse géologique du Sud-Est de la France. Atlas. - Mém. BRGM. 126.
- FISCHER, G. & P.-A. SCHNEGG, 1979: Carte de la déclinaison en Suisse. Epoque 1978.0. Echelle 1:500'000. Swiss Geophys. Comm.
- FISCHER, G. & P.-A. SCHNEGG, 1979: Carte de l'inclinaison en Suisse. Epoque 1978.0. Echelle 1:500'000. Swiss Geophys. Comm.

- FISCHER, G. & P.-A. SCHNEGG, 1979: Carte de l'intensité totale en Suisse. Epoque 1978.0. Echelle 1:500'000. Swiss Geophys. Comm.
- KLINGELE, E.E., 1983: Carte aéromagnétique (Intensité totale) du Plateau et du Jura Suisse. Epoque 1980.5. Altitude de vol 1829 m.s.m. Echelle 1:500'000. Swiss Geophys. Comm.
- KLINGELE, E.E., 1986: Les levés aéromagnétiques de la Suisse. Geodätisch-geophysikalische Arbeiten in der Schweiz. 69 pages. Swiss Geodetic Comm.

- KLINGELE, E.E., & ST. MUELLER, 1987: La cartographie du soubassement magnétique du bassin molassique et du Jura Suisse. *Eclogae geol. Helv.* 80/1, 17–36.
- LAUBSCHER, H.P., 1972: Some overall aspects of Jura dynamics. *Amer. Sci* 272, 293–304
- GREEN, R. & STANLEY, I.M., 1975: Application of a Hilbert transform method to the interpretation of surface vehicle magnetic data. *Geophys. Prospect.* 23, 18–27.
- NABIGHIAN, M. N., 1972: The analytic signal of two-dimensional bodies with polygonal cross-section: Its properties and use for automated anomaly interpretation: *Geophysics* 37, 507–527.
- NABIGHIAN, M. N., 1974: Additional comments on the analytic signal of two-dimensional magnetic bodies with polygonal cross-section: *Geophysics* 39, 85–92.
- NABIGHIAN, M. N., 1984: Toward a three-dimensional automatic interpretation of potential field data via generalised Hilbert transforms: *Fundamental relations: Geophysics* 49, 80–91.
- REID, A. B., ALLSOP, J.M., GRANSER, H., MILLET, A.J. & SOMERTON, I.W., 1990: Magnetic interpretation in three dimension using Euler deconvolution: *Geophysics* 55, 80–91.
- RISNES, K., DUMONT, B., OLIVIER, R. & WAGNER, J.-J. 1993: Etude des anomalies magnétiques et gravimétriques de la région du Chasseral. *Mat. Géol. Suisse, série Géophysique*, No 26. Swiss Geophysical Commission.
- TALWANI, M. & HEIRTZLER, J.R., 1964: Computation of magnetic anomalies caused by two-dimensional structures of arbitrary shape, in: *Computers in the mineral industry, part 1: Stanford University Publications, Geological Sciences* 9, 464–480.
- THOMPSON, D.T., 1982: EULDPH: A new technique for making computer-assisted depth estimation from magnetic data: *Geophysics* 47, 31–37.
- TREITEL, S., CLEMENT, W.G. & KAUL, R.K., 1971: The spectral determination of depths to buried magnetic basement rocks. *Geophys. J. R. Astronom. Soc.* 24, 415–428.

Manuscript received September 3, 2002  
 Revision accepted February 22, 2003

